

# Supporting Information for “Tectonic Evolution of the Condrey Mountain Schist: an Intact Record of Late Jurassic to Early Cretaceous Franciscan Subduction and Underplating”

C. M. Tewksbury-Christle<sup>1</sup>, W. M. Behr<sup>2</sup>, M. A. Helper<sup>3</sup>, and D. F. Stockli<sup>3</sup>

<sup>1</sup>Geosciences Department, Fort Lewis College, 1000 Rim Drive, Durango, CO, 81301

<sup>2</sup>Structural Geology and Tectonics Group, Geological Institute, Department of Earth Sciences, ETH Zurich, Sonneggstrasse 5, 8092 Zurich, Switzerland

<sup>3</sup>Department of Earth and Planetary Sciences, Jackson School of Geosciences, University of Texas at Austin, 2305 Speedway Stop C1160, Austin, TX 78712

## Contents of this file

1. Figures S1 to S6

### Additional Supporting Information (Files uploaded separately)

1. Captions for Data Sets DS1 to DS7

**Introduction.** This supporting information file includes additional figures that are referenced in the text. For the purposes of peer review, the supporting data sets have been uploaded along with the manuscript. If the manuscript is accepted for publication, we will upload these data sets to the ETH Research Collection, which will allow for public access and will index the datasets with a DOI.

### Figures S1 to S6

The supporting figures for this article along with their captions are included on pages X-3 through X-8.

### Captions for Data Sets DS1 to DS7

**Dataset S1.** U-Pb magmatic zircon age data collected by Helper and N. Walker in 1988, unpublished. All locations are reported using NAD83, UTM 10N. <sup>1</sup>NM = nonmagnetic fraction; M = magnetic fraction; DM = diamagnetic fraction; NDM = nondiamagnetic fraction; f = fine-grained fraction; c = coarse-grained fraction. \*Denotes radiogenic Pb (corrected for non-radiogenic initial and Pb blank). Non-radiogenic Pb is estimated to have an isotopic composition of 204:206:207 = 1:18.8:15.6. The composition of non-radiogenic Pb introduces little uncertainty to the calculated ages due to the magnitude of the zircon <sup>206</sup>Pb/<sup>204</sup>Pb. <sup>2</sup>Ratios have been corrected for mass fractionation based on replicate analyses of NBS SRM 981 and SRM 983. Uncertainty (at the two-sigma level) of the measured ratio is better than 0.2% for <sup>208</sup>Pb/<sup>206</sup>Pb, better than 0.1% for <sup>207</sup>Pb/<sup>206</sup>Pb, and ranges from 0.1% to 4% for <sup>206</sup>Pb/<sup>204</sup>Pb. <sup>3</sup>Decay constants: <sup>238</sup>U = 1.55125E-10; <sup>235</sup>U = 9.8485E-10. Atomic ratio of <sup>238</sup>U/<sup>235</sup>U =

137.88. Uncertainty in the ages is stated at the two-sigma level. Uncertainty in the <sup>206</sup>Pb/<sup>238</sup>U age is based on combined uncertainties in the <sup>206</sup>Pb and <sup>238</sup>U concentration determinations and reproducibility of NBS SRM 981, SRM 983 and SRM U500. Uncertainty in the <sup>207</sup>Pb/<sup>206</sup>Pb ages is based on the combined uncertainties in the measurement of the zircon <sup>207</sup>Pb/<sup>206</sup>Pb and <sup>206</sup>Pb/<sup>204</sup>Pb ratios, estimated uncertainty in the <sup>207</sup>Pb/<sup>204</sup>Pb ratio of non-radiogenic Pb (assumed to be +0.2), and reproducibility of the NBS standards. Uncertainty in the <sup>207</sup>Pb/<sup>235</sup>U age is derived from combined uncertainties in the <sup>206</sup>Pb/<sup>238</sup>U and <sup>207</sup>Pb/<sup>206</sup>Pb ratios.

**Dataset S2.** MDAs calculated using the youngest single grain (YSG), youngest 2 or more grains that overlap at 1 $\sigma$  (YC1 $\sigma$ ), and youngest 3 or more grains that overlap at 2 $\sigma$  (YC2 $\sigma$ ). N is the number of concordant grains, and n is the number of grains used to define the MDA. Each tab has all data for individual samples, and ages are summarized here based on youngest single grain (YSG), youngest 2 or more that overlap at 1 $\sigma$ (YC1 $\sigma$ ), and youngest 3 or more grains that overlap at 2 $\sigma$ (YC2 $\sigma$ ).

**Dataset S3.** K-Ar dates on white mica from F. McDowell’s Lab, 1988-89, unpublished. Constants used:  $\lambda_B = 4.963\text{e-}10/\text{yr}$ ;  $\lambda_e + \lambda' = 0.581\text{e-}10/\text{yr}$ ;  $^{40}\text{K}/\text{K} = 1.167\text{e-}4$ . All locations are reported using NAD83, UTM 10N. Samples highlighted with gray backgrounds are amphibole K-Ar ages. The rest are white mica K-Ar ages.

**Dataset S4.** Rb-Sr dates from M. Helper, 1987-89, unpublished. All locations are reported using NAD83, UTM 10N. \*Separates denoted with an astericks were treated with 10% HCl prior to chemical separation of Rb and Sr. <sup>1</sup>Concentrations were measured by isotope dilution using a mixed <sup>87</sup>Rb and <sup>84</sup>Sr spike. Analytical uncertainty is  $\pm 1.5\%$  (1 $\sigma$ ) of these values. <sup>2</sup>1 $\sigma$  uncertainty for <sup>87</sup>Sr/<sup>86</sup>Sr values based on replicate analyses of rock standard BCR-1 is 0.008%. Analyses of NBS 987 during the period of this work gave <sup>87</sup>Sr/<sup>86</sup>Sr of 0.71023(6) (2 $\sigma$ ). All values were fractionation corrected

assuming  $^{86}\text{Sr}/^{88}\text{Sr}=0.1194$ .  $^3$ Isochron dates, initial ratios, uncertainties and MSWDs are from the online IsoplotR program (v. 4.1) using Model 1 and default inputs for Rb and Sr isotopic ratios and the Rb decay constant.  $^4$ Initial  $^{87}\text{Sr}/^{86}\text{Sr}$  ratio uncertainties are expressed within brackets, e.g. 0.70397(3) is  $0.70397 \pm 0.00003$ .

**Data Set S5.** Raman spectra from lower CMS samples were collected on ETH Zurich's DILOR Labram micro-Raman spectrometer. Peak locations and areas are from Igor Pro peak fitting and temperature was calculated using Beyssac, Goffé, Chopin, and Rouzaud (2002)'s temperature calibration. All sample locations are in decimal degrees.

**Data Set S6.** Si-in-Phengite data were collected using ETH Zürich's JEOL JXA-8230 Electron Probe Microanalyser. The first tab lists the standards used for Si-in-phengite analyses. All standards are listed in ETH Zurich's Electron Microprobe Database. Following tabs

list Si p.f.u. calculated for different locations and deformation phases and under different assumptions.

**Data Set S7.** Each tab contains trace element data measured on grains for CT-CMW36 and CT-CMW53. Corresponding U/Pb data and ages are in DS02.

## References

- Beyssac, O., Goffé, B., Chopin, C., & Rouzaud, J. N. (2002). Raman spectra of carbonaceous material in metasediments: a new geothermometer. *Journal of Metamorphic Geology*, *20*, 859–871. doi: 10.1046/j.1525-1314.2002.00408.x
- Sharman, G. R., Graham, S. A., Grove, M., Kimbrough, D. L., & Wright, J. E. (2015). Detrital zircon provenance of the Late Cretaceous-Eocene California forearc: Influence of Laramide low-angle subduction on sediment dispersal and paleogeography. *Bulletin*, *127*(1-2), 38–60. doi: 10.1130/B31065.1

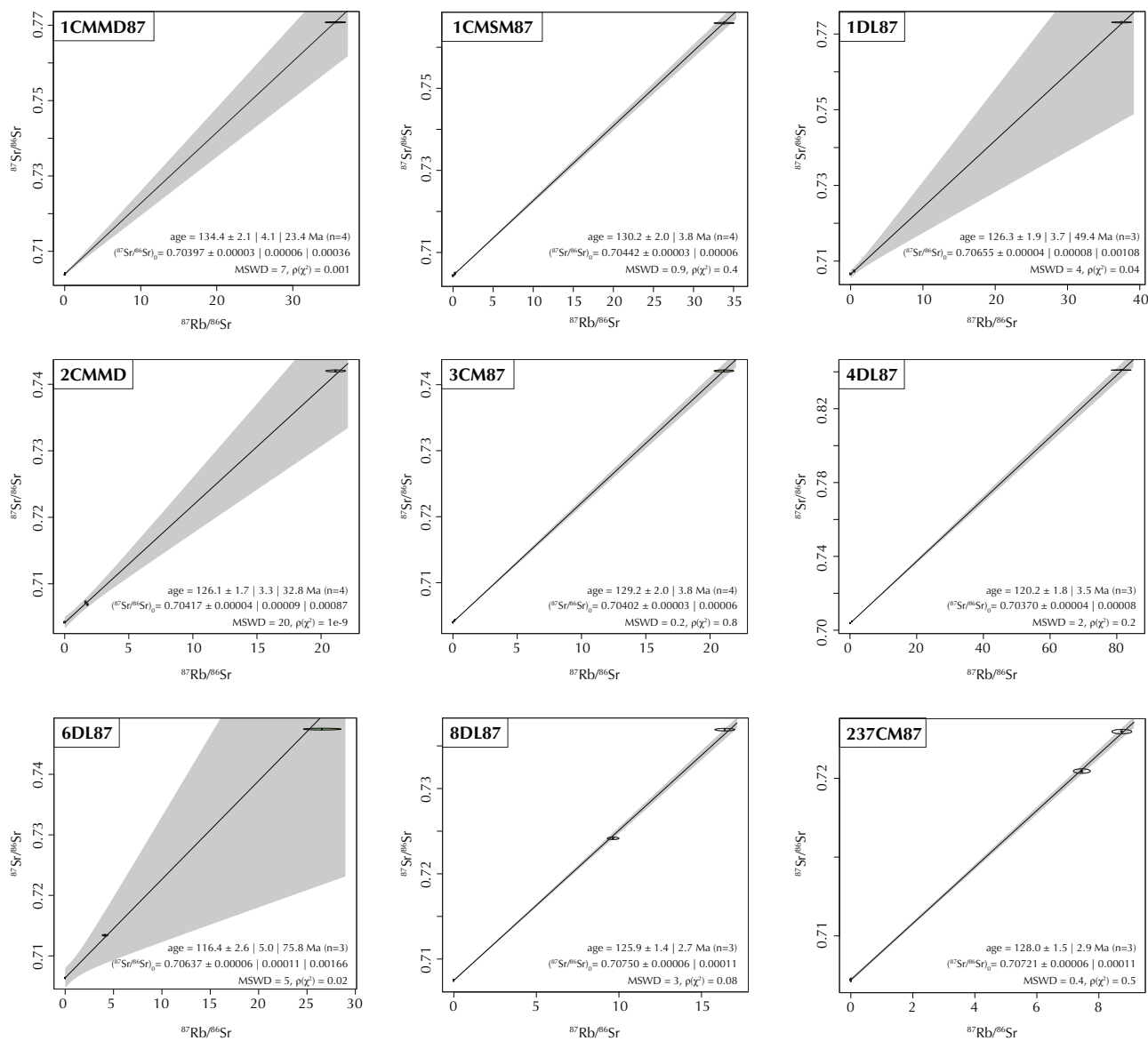


**Figure S1.** Multimineral isochrons for Rb-Sr samples. All ages are calculated for apatite-whole rock-phengite isochrons except for 4DL87, which used a titanite-whole rock-phengite isochron. Sample locations and data are in DS04.

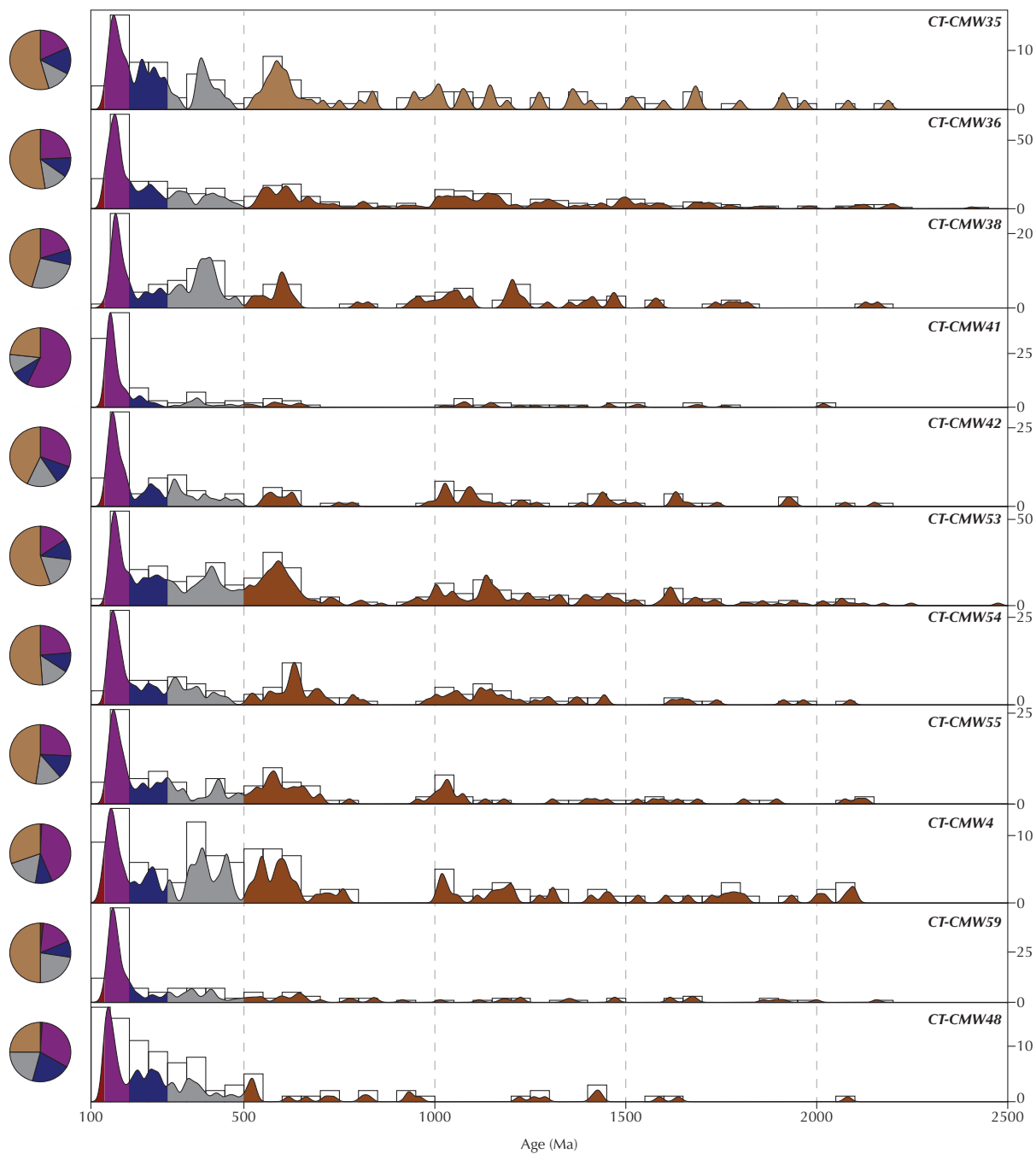


**Figure S2.** Kernel Density Estimations (KDEs) for the lower CMS detrital zircon data. Color bins follow Sharman et al. (2015). Samples are organized with increasing structural depth from top to bottom. Pie charts show relative proportions of samples binned by 100-135 Ma (red), 135-200 Ma (purple), 200-300 (navy), 300-500 (gray), and 500+ (tan).

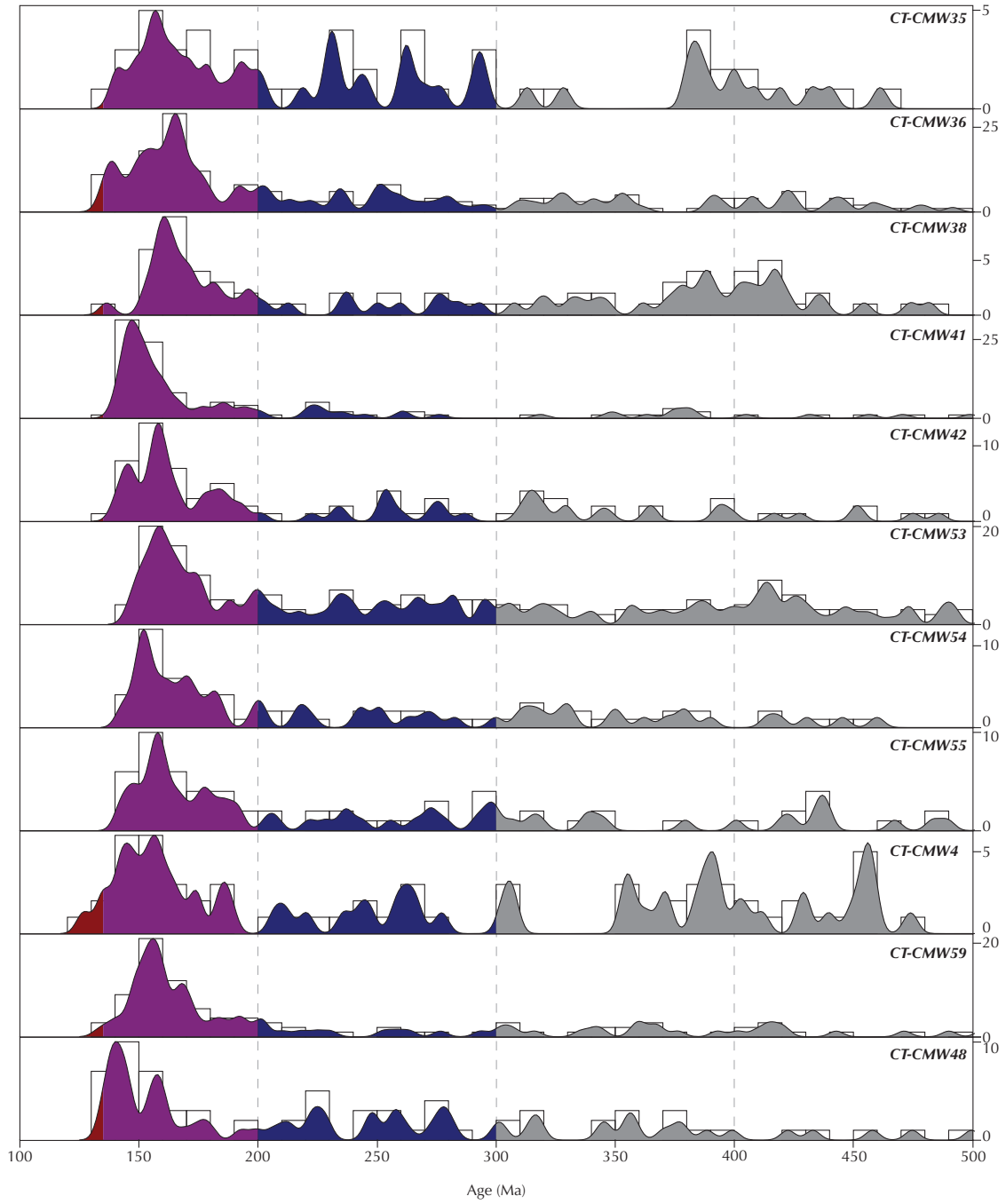
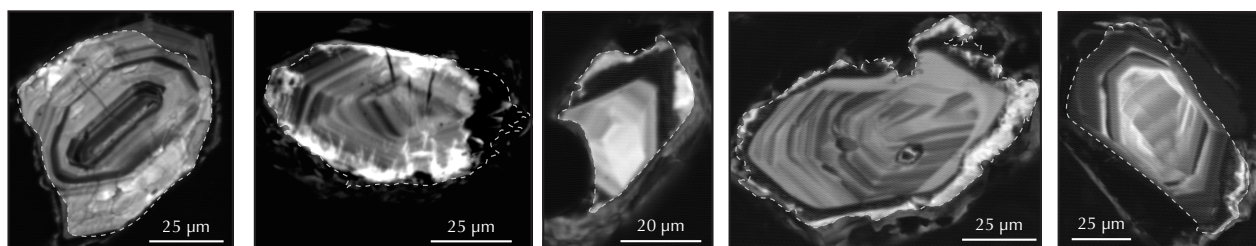


**Figure S3.** Kernel Density Estimations (KDEs) for the lower CMS detrital zircon data over 100-500 Ma. Color bins follow Sharman et al. (2015) and Fig. S2. Samples are organized with increasing structural depth from top to bottom.

**a** CT-CMW35



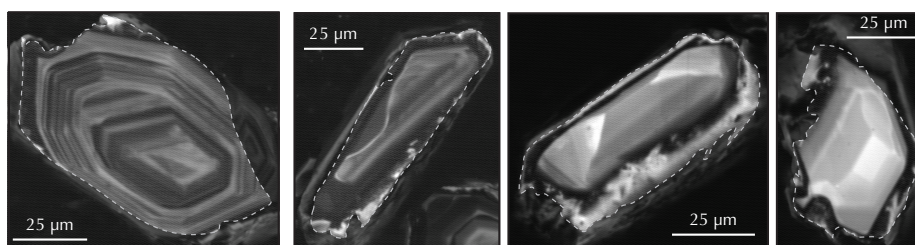
rim:  $140.1 \pm 3.2$  Ma  
core:  $172 \pm 2.9$  Ma (D)

rim:  $144 \pm 18$  Ma (D)  
core:  $539.0 \pm 6.6$  Ma

$148.2 \pm 2.1$  Ma

$164.8 \pm 1.4$  Ma

$186.1 \pm 2.2$  Ma



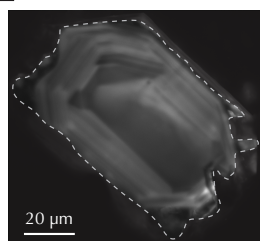
$230.0 \pm 1.8$  Ma

$241.8 \pm 3.1$  Ma

$269.7 \pm 3.3$  Ma

$276.6 \pm 5.5$  Ma

**b** CT-CMW55



rim:  $131.7 \pm 7.8$  Ma  
core:  $158.8 \pm 1.7$  Ma

**Figure S4.** Additional CL images of grains from CT-CMW35 (a) and CT-CMW55 (b). All other images are presented in the main manuscript text. Bright white amorphous zones at the margins of grains in CT-CMW35 is tape residue.

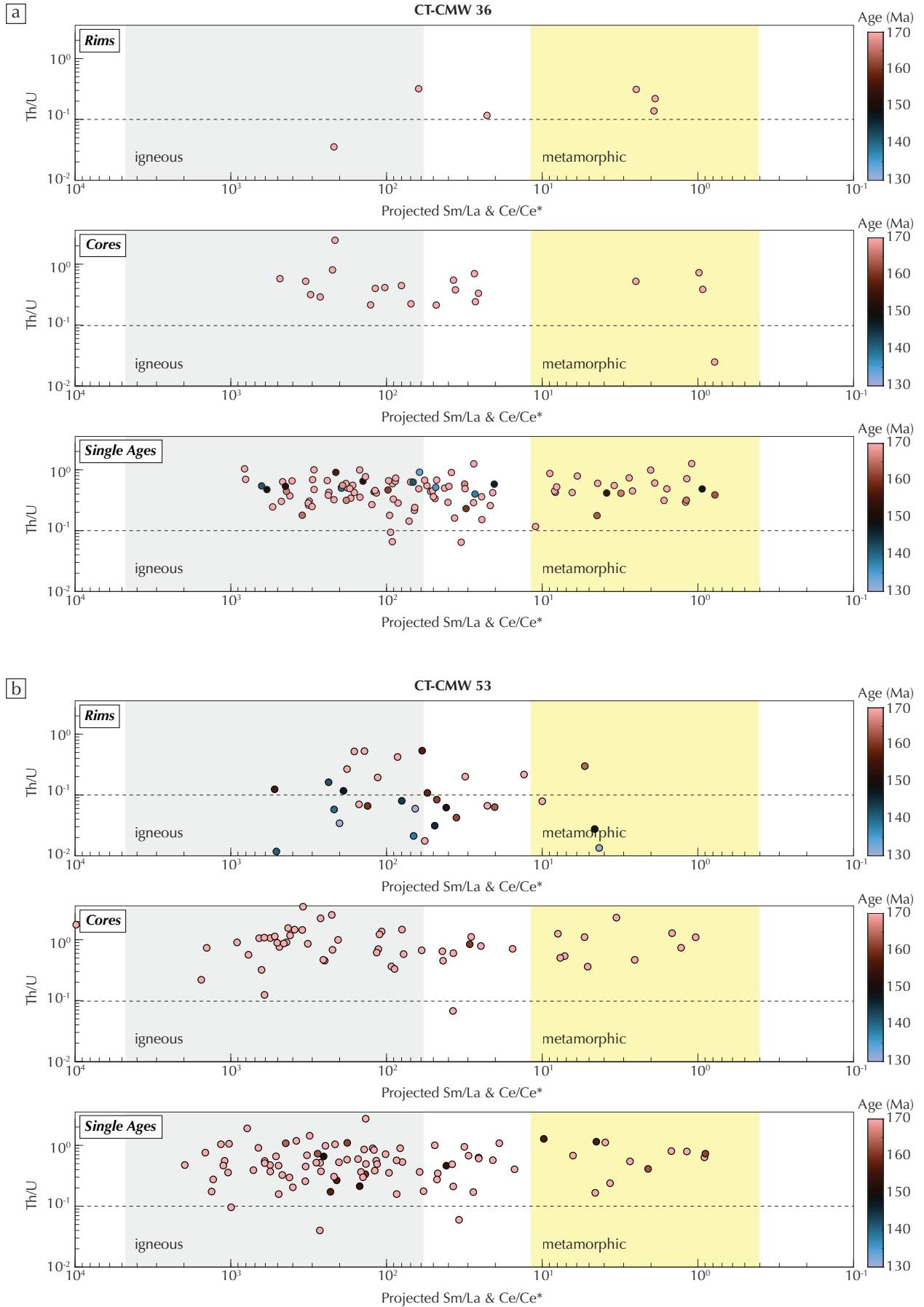


**Figure S5.** Ce/Ce\* and Sm/La values and fields (gray and yellow) projected onto a single axis using principle component analysis in order to plot versus Th/U for CT-CMW36 (a) and CT-CMW53 (b). Age shown by colors of the symbols. Dashed line indicates Th/U = 0.1.

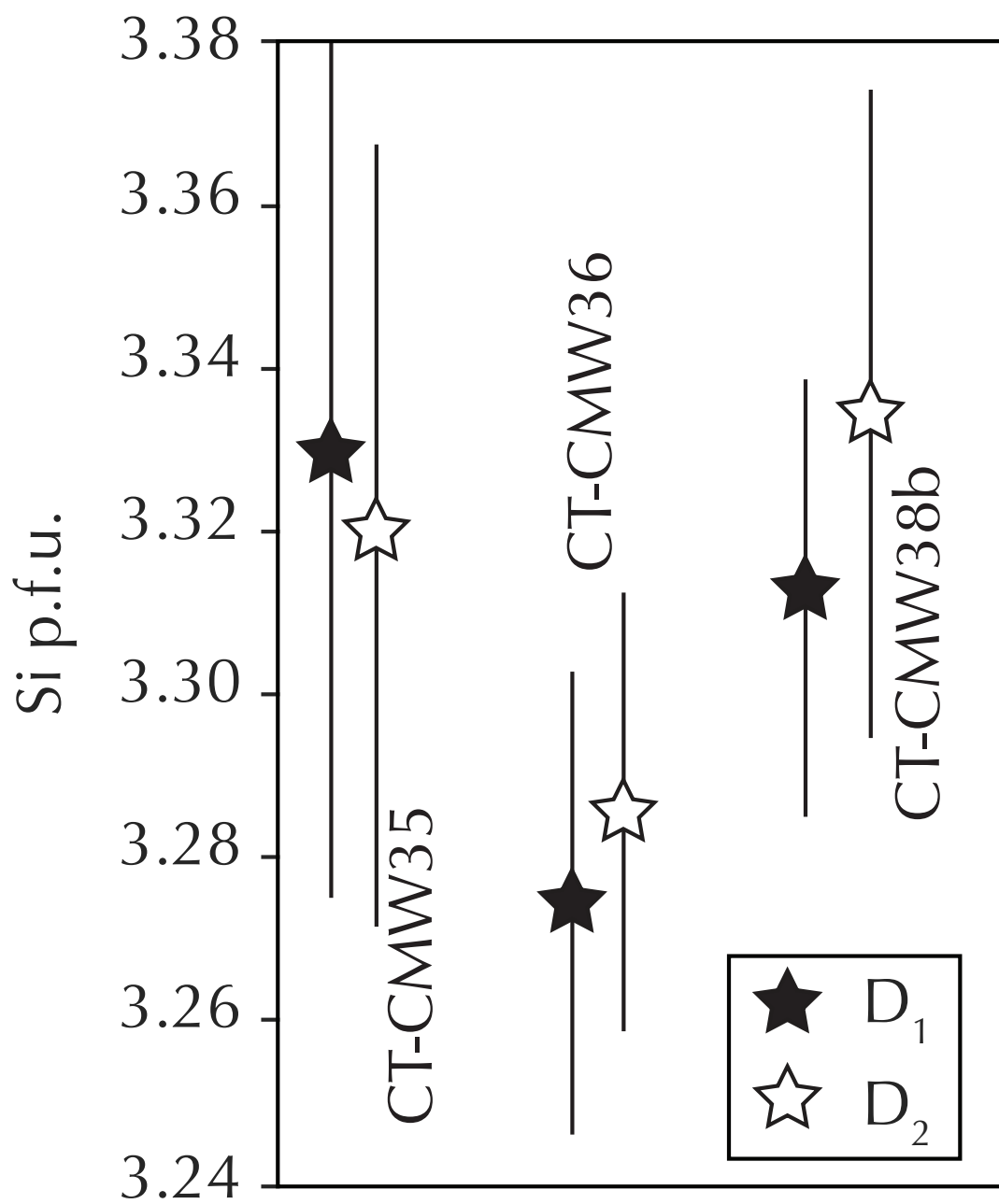


**Figure S6.** Si per formula unit in D<sub>1</sub> and D<sub>2</sub> white micas for representative samples. Si-in-phengite measurements were taken at ETH Zurich on the JEOL JXA-8230 Electron Probe Microanalyser. Sample locations are listed in Data Set S6.